

G.E. Volovik

On Larkin-Imry-Ma State of $^3\text{He-A}$ in Aerogel

01.10.2007

Keywords superfluid ^3He , disorder and porous media

Abstract Superfluid $^3\text{He-A}$ shares the properties of spin nematic and chiral orbital ferromagnet. Its order parameter is characterized by two vectors $\hat{\mathbf{d}}$ and $\hat{\mathbf{l}}$. This doubly anisotropic superfluid, when it is confined in aerogel, represents the most interesting example of a system with continuous symmetry in the presence of random anisotropy disorder. We discuss the Larkin-Imry-Ma state, which is characterized by the short-range orientational order of the vector $\hat{\mathbf{l}}$, while the long-range orientational order is destroyed by the collective action of the randomly oriented aerogel strings. On the other hand, sufficiently large regular anisotropy produced either by the deformation of the aerogel or by applied superflow suppresses the Larkin-Imry-Ma effect leading to the uniform orientation of $\hat{\mathbf{l}}$. The interplay of regular and random anisotropy allows us to study many different effects.

PACS numbers: 61.30.-v, 67.57.-z, 75.10.Nr.

1 Introduction

NMR experiments on liquid ^3He confined in aerogel demonstrate a rich but still unexplained life in two regions of the phase diagram in Fig. 1: (i) in the region between the lines T_{cb} and T_{ca} of superfluid phase transition in bulk liquid and in aerogel correspondingly¹ (in principle, Berezinskii odd-frequency pairing state is possible there²); and (ii) in the region of the so-called A-like phase which is metastable in the absence of external magnetic field^{3,4,5}. Here we concentrate on the A-like phase, which will be discussed in terms of the Larkin-Imry-Ma effect occurring in the anisotropic $^3\text{He-A}$ superfluid when it is confined in aerogel.

Low Temperature Laboratory, Helsinki University of Technology, P.O.Box 2200, FIN-02015 HUT, Finland, and L.D. Landau Institute for Theoretical Physics, 119334 Moscow, Russia
Tel.: 358-9-4512963
Fax: 358-9-4512969
E-mail: volovik@boojum.hut.fi

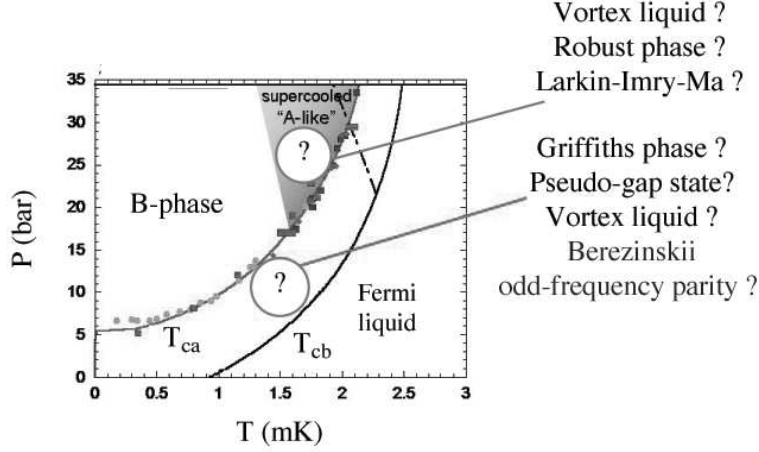


Fig. 1 Two main problems for superfluid ^3He in aerogel: (1) What is the state of ^3He between two lines of superfluid phase transition? What is the state of ^3He in the so-called A-like phase?

1.1 Doubly anisotropic superfluid ^3He -A

Superfluid ^3He -A shares the properties of spin nematic and chiral orbital ferromagnet. Its order parameter is characterized by two vectors $\hat{\mathbf{d}}$ and $\hat{\mathbf{l}}^6$:

$$A_{\mu i} = \Delta e^{i\phi} \hat{d}_\mu (\hat{m}_i + i\hat{n}_i) , \quad \hat{\mathbf{l}} = \hat{\mathbf{m}} \times \hat{\mathbf{n}} . \quad (1)$$

Unit vector $\hat{\mathbf{d}}$ marks direction of anisotropy axis in spin space, and is responsible for anisotropy of spin susceptibility; unit vector $\hat{\mathbf{l}}$ marks the direction of the orbital angular momentum of Cooper pairs and simultaneously the direction of axis of the orbital anisotropy and it is responsible for anisotropy of superfluid density:

$$F_s + F_o + F_{so} = \frac{(\mathbf{S} \cdot \hat{\mathbf{d}})^2}{2\chi_{\parallel}} + \frac{(\mathbf{S} \times \hat{\mathbf{d}})^2}{2\chi_{\perp}} + \frac{\rho_{s\parallel}}{2} (\mathbf{v}_s \cdot \hat{\mathbf{l}})^2 + \frac{\rho_{s\perp}}{2} (\mathbf{v}_s \times \hat{\mathbf{l}})^2 - g_D (\hat{\mathbf{d}} \cdot \hat{\mathbf{l}})^2 . \quad (2)$$

Here \mathbf{S} is spin density in the applied magnetic field, $S_\alpha = \chi_{\alpha\beta} H_\beta$; \mathbf{v}_s is the velocity of superfluid mass current $j_s^i = \rho_s^{ij} v_s^j$. Because of the chiral nature of the orbital order parameter $\hat{\mathbf{m}} + i\hat{\mathbf{n}}$, the superfluid velocity and its vorticity

$$\mathbf{v}_s = \frac{\hbar}{2m} (\nabla\phi + \hat{m}_i \nabla \hat{n}_i) , \quad \nabla \times \mathbf{v}_s = \frac{\hbar}{4m} e^{ijk} \hat{l}_i \nabla \hat{l}_j \times \nabla \hat{l}_k , \quad (3)$$

can be generated by the texture of the $\hat{\mathbf{l}}$ -vector⁷. The last term in Eq.(2) describes a tiny spin-orbit coupling F_{so} between $\hat{\mathbf{d}}$ and $\hat{\mathbf{l}}$, which is however very important for the NMR measurements since it produces the frequency shift.

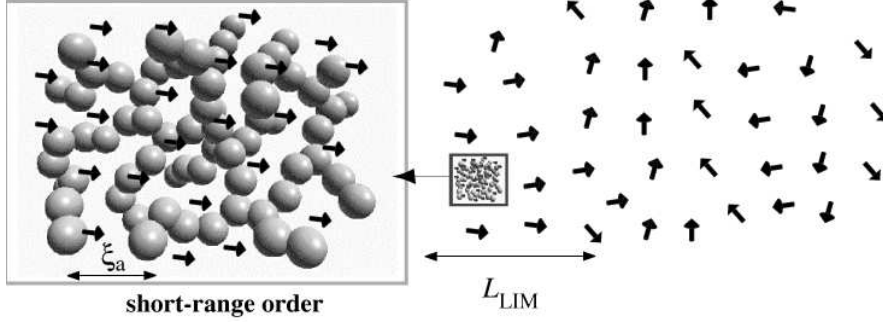


Fig. 2 While the short-range order is well defined, the collective orientational effect of aerogel strings destroys the long-range order on a macroscopic Larkin-Imry-Ma scale L_{LIM}

This doubly anisotropic superfluid, when it is confined in aerogel, represents the most interesting example of a system with continuous symmetry in the presence of random anisotropy. For such systems the surprising conjecture was made by Imry and Ma⁸ that even a weak disorder may destroy the long-range orientational order (LRO). This is the counterpart of the effect of collective pinning in superconductors predicted by Larkin⁹, in which weak impurities destroy the long-range translational order of the Abrikosov vortex lattice. Recent NMR experiments allow us to discuss the state of $^3\text{He-A}$ in aerogel in terms of the Larkin-Imry-Ma (LIM) state. The LIM state in $^3\text{He-A}$ is characterized by short-range orientational order of the orbital vector $\hat{\mathbf{l}}$, while the LRO is destroyed by the collective action of the randomly oriented aerogel strings (Fig. 2). The order of magnitude theoretical estimations based on the model of aerogel in Sec. 2.1 and the NMR data suggest that in the aerogel samples under investigation, the LIM length L_{LIM} at which the LRO is destroyed is of order of a micron.

Though L_{LIM} is much bigger than the microscopic scales of aerogel strands, the orientational disorder may have pronounced effects. In particular, it may be the reason of existence of a small region of equilibrium A-phase in zero magnetic field¹⁰. For NMR experiments it is important that L_{LIM} is smaller than dipole length $\xi_D \sim 10 \mu\text{m}$ characterizing spin-orbit coupling between $\hat{\mathbf{l}}$ and $\hat{\mathbf{d}}$ in Eq.(2). This leads to anomalously small values of the observed transverse NMR frequency shift and longitudinal NMR frequency³ as we shall discuss in Sec. 3.

A regular anisotropy may suppress the LIM effect, and this does take place when one applies a uniaxial deformation to the aerogel sample (Sec. 2.2). A linear deformation of about 1% leads to the restoration of the uniform orientation of the $\hat{\mathbf{l}}$ -vector in the sample⁴. As a result the value of the transverse NMR frequency shift is enhanced by an order of magnitude compared to that in the LIM state. If the deformation leads to orientation of $\hat{\mathbf{l}}$ along the magnetic field \mathbf{H} , the transverse NMR frequency shift becomes negative. These are the observations which support the interpretation of the A-phase like state in aerogel as the disordered LIM state.

Open problems related to the disordered LIM state including the superfluid properties of the LIM state are discussed in Sec. 4. Superfluidity in LIM state could be rather unusual because, according to the Mermi-Ho relation in Eq.(3) between $\hat{\mathbf{l}}$ and \mathbf{v}_s , the LIM texture generates superfluid vorticity. As a result, the disordered LIM state can be represented as a system of randomly distributed skyrmions –

vortices with continuous cores. The characteristic distance between the vortex-skyrmions and the size of their cores are determined by the LIM length L_{LIM} . In principle, the superfluid density of $^3\text{He-A}$ in aerogel may depend on the ability of the aerogel to pin the randomly distributed vortex-skyrmions.

2 Theory of Larkin-Imry-Ma effect

2.1 Larkin-Imry-Ma state in the model of random cylinders

We use a simple model of aerogel as a system of randomly oriented cylindrical strands (see Refs.^{11,12} and Fig. 3 *middle*) with diameter $\delta \sim 3$ nm and length $\xi_a \sim 20$ nm, which is also the distance between strands. Since δ is much smaller than the superfluid coherence length ξ_0 , the theory of Rainer and Vuorio for the microscopic body immersed in $^3\text{He-A}$ ¹³ can be applied. According to¹³ the $\hat{\mathbf{I}}$ -vector remains uniform outside the body (see Fig. 2 *left*), and the orientational energy acting from $\hat{\mathbf{I}}$ on a cylinder i with the direction of axis along $\hat{\mathbf{n}}_i$ is

$$E_i = E_a(\hat{\mathbf{I}} \cdot \hat{\mathbf{n}}_i)^2, \quad E_a \sim \frac{\Delta^2}{T_c} k_F^2 \xi_a \delta > 0. \quad (4)$$

Here k_F is Fermi momentum; the parameter E_a is positive as follows from¹³.

For the infinite system of cylinders, the average orientational effect of the random cylinders on the $\hat{\mathbf{I}}$ -vector is absent, if the $\hat{\mathbf{I}}$ -vector is kept uniform. However, there is a collective effect of many cylinders, which makes the $\hat{\mathbf{I}}$ -vector inhomogeneous on large scales. Let us consider the box of size $L \times L \times L$, which contains a large but finite number $N \sim L^3/\xi_a^3 \gg 1$ of randomly oriented cylinders and still has a uniform orientation of the $\hat{\mathbf{I}}$ -vector. Due to fluctuations of orientational energies of randomly oriented cylinders, the $\hat{\mathbf{I}}$ -vector will find the preferred orientation in the box, with the energy gain proportional to $N^{1/2}$. The corresponding negative energy density is determined by the variance of the energy of random anisotropy:

$$E_{\text{ran}} \sim - \left\langle \sum_{i=1}^N (E_i - \langle E \rangle)^2 \right\rangle^{1/2} L^{-3} \sim -N^{1/2} E_a L^{-3} \sim -E_a \xi_a^{-3/2} L^{-3/2}. \quad (5)$$

The neighboring boxes prefer different orientations of $\hat{\mathbf{I}}$, as a result the effect of orientation by the aerogel strands will be opposed by the gradient energy $E_{\text{grad}} \sim K(\nabla \hat{\mathbf{I}})^2 \sim K/L^2$. The optimal size of a box with a uniform orientation of $\hat{\mathbf{I}}$ within the box – the LIM length L_{LIM} at which LROO is destroyed – is found from competition between the energy of random anisotropy and the gradient energy:

$$E_{\text{ran}} + E_{\text{grad}} \sim -E_a \xi_a^{-3/2} L^{-3/2} + KL^{-2}. \quad (6)$$

Minimization of Eq.(6) gives

$$L_{\text{LIM}} \sim \frac{K^2 \xi_a^3}{E_a^2} \sim \xi_a \frac{\xi_0^2}{\delta^2}. \quad (7)$$

Here we used Eq.(4) for E_a ; and estimated the rigidity of $\hat{\mathbf{I}}$ as $K \sim (k_F^3/m)(\Delta^2/T_c^2)$.

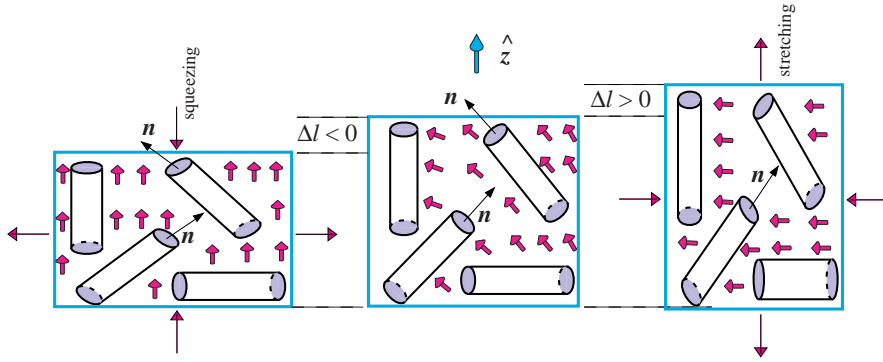


Fig. 3 Uniaxial deformation of cylindrical sample of aerogel. Squeezing (stretching) of cylinder along its axis z leads to global anisotropy for $\hat{\mathbf{I}}$ with easy axis along z (easy plane normal to z)

Eq.(7) is valid for thin strings, $\delta \ll \xi_0$. This corresponds to collective pinning: $\hat{\mathbf{I}}$ is not pinned by individual strings, has a short-range orientational order and is perfectly uniform at the aerogel scale ξ_a . The LRO is lost at scale $L_{\text{LIM}} \gg \xi_a$ due to collective effect of many strings (Fig. 2 right). With $\xi_a \sim \xi_0 \sim 20$ nm and $\delta \sim 3$ nm, the length $L_{\text{LIM}} \sim 1$ μm . Strong pinning would occur in case of thick strings, $\delta > \xi_0$, when $\hat{\mathbf{I}}$ is oriented by each string due to boundary conditions for $\hat{\mathbf{I}}$ at the surface of a string, and the LRO is destroyed at the scale of ξ_a .

2.2 LIM effect killed by regular anisotropy

Squeezing of a cylindrical sample of aerogel along its axis ($u_{zz} \sim \Delta l/l < 0$, Fig. 3 left) makes z the easy axis for $\hat{\mathbf{I}}$, while stretching ($u_{zz} \sim \Delta l/l > 0$, Fig. 3 right) produces the easy plane anisotropy. In general, the deformation u_{ik} of aerogel induces regular anisotropy for the $\hat{\mathbf{I}}$ -vector with the density of orientational energy:

$$E_{\text{reg}} = \left\langle \sum_i (E_i - \langle E \rangle) \right\rangle = \kappa \left(u_{ik} - \frac{1}{3} u_{ll} \delta_{ik} \right) \hat{l}_i \hat{l}_k, \quad \kappa \sim E_a \xi_a^{-3}. \quad (8)$$

Comparing this energy with the LIM energy (in Eq.(6) at $L = L_{\text{LIM}}$), one finds that the ordered state with $\hat{\mathbf{I}}$ oriented along the easy axis $\hat{\mathbf{z}}$ becomes more energetically favorable than the LIM state when the squeezing is sufficiently large:

$$\frac{|\Delta l|}{l} > \left(\frac{\xi_a}{L_{\text{LIM}}} \right)^{3/2}. \quad (9)$$

In the weak pinning limit of $^3\text{He-A}$ in aerogel the LIM effect is so subtle, that the critical value of the deformation at which the first order phase transition from the LIM state to the uniform state occurs is rather small; $\Delta l/l \sim 10^{-3} - 10^{-2}$. For large stretching the polar phase is predicted to appear in vicinity of T_{ca} ¹⁴. Experimentally, squeezing by about 1% is enough to get the uniform $\hat{\mathbf{I}}$ texture⁴. On the other hand, recent experiments¹⁵ in which compression has been applied to compensate intrinsic deformations, indicate that when the deformation becomes below 1%, the initial uniform $\hat{\mathbf{I}}$ texture is transformed to the disordered state.

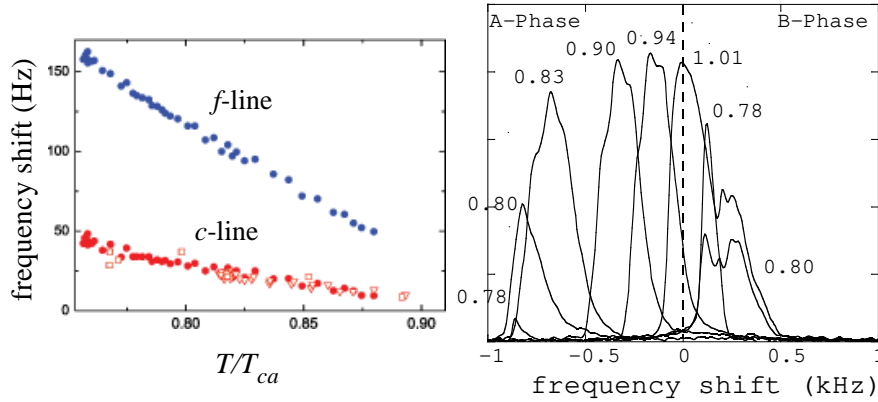


Fig. 4 *left*: Temperature dependence of positive frequency shift for two lines observed in NMR spectrum on $^3\text{He-A}$ in aerogel sample according to Ref.³ ($P = 29.3$ bar, $H = 224$ G). *right*: Negative frequency shift in the NMR spectrum observed in $^3\text{He-A}$ in deformed aerogel according to Ref.⁴ ($P = 29.3$ bar, $H = 290$ G)

3 Experiment

3.1 Estimation of Larkin-Imry-Ma length from NMR

Fig. 4 demonstrates results of the NMR experiments on $^3\text{He-A}$ in conventional aerogel sample³ (*left*), and in a squeezed aerogel⁴ (*right*). In the latter, the transverse NMR line has negative frequency shift corresponding to the uniform $\hat{\mathbf{l}}$ -vector oriented along the magnetic field $\mathbf{H} \parallel \hat{\mathbf{z}}$.

In Ref.³ two NMR lines have been observed in the transverse NMR spectrum in Fig. 4 (*left*). The line with a larger frequency shift, denoted as *f*-line, can be removed after application of the 180° pulse while cooling through T_{ca} (the superfluid transition temperature in aerogel). The salient feature of the *c*-line which survives after the 180° pulse is the anomalously small frequency shift. It is about 30 times smaller than the magnitude of the negative frequency shift observed in Refs.^{4,5} in the aerogel sample with the uniform $\hat{\mathbf{l}}$ -vector (we take into account that the frequency shift is $\propto 1/H$ with $H = 224$ G in Ref.³ and $H = 290$ G in Ref.⁴). This large difference can be easily understood if one identifies the *c*-state (the state with a single *c*-line in the spectrum) as the LIM state.

Properties of NMR on the LIM state depend on ratio between L_{LIM} and the dipole length $\xi_D \sim 10 \mu\text{m}$ of spin-orbit coupling between $\hat{\mathbf{l}}$ and $\hat{\mathbf{d}}$. The orbital vector $\hat{\mathbf{l}}$ will be locked with the spin-space vector $\hat{\mathbf{d}}$ if $L_{\text{LIM}} > \xi_D$ and unlocked from $\hat{\mathbf{d}}$ if $L_{\text{LIM}} < \xi_D$. The NMR results are in favor of the almost completely unlocked case, since in the limit $L_{\text{LIM}}/\xi_D \ll 1$, the $\hat{\mathbf{l}}$ -texture is fully disordered, $\langle l_z^2 \rangle = 1/3$, and the frequency shift is zero¹⁶. The nonzero but relatively small magnitude of the frequency shift compared to the negative frequency shift, $\Delta\omega_{c\text{-line}} \sim |\Delta\omega_{\text{deformed}}|/30$, can be ascribed to the $(L_{\text{LIM}}/\xi_D)^2$ correction. This allows us to estimate $L_{\text{LIM}} \sim 1 \mu\text{m}$, which is in a reasonable agreement with Eq.(7).

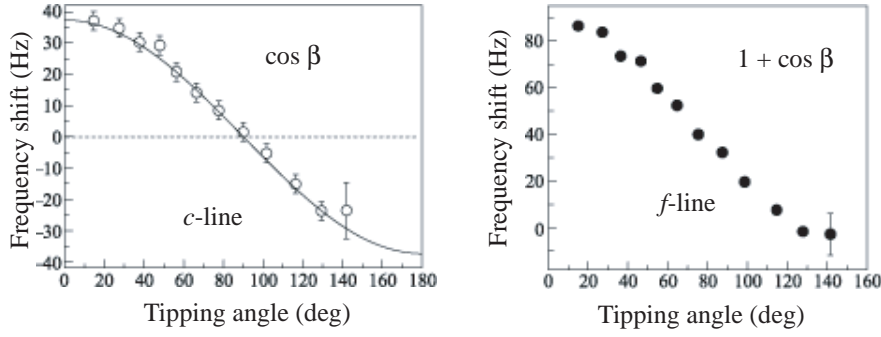


Fig. 5 Tipping angle dependence of the frequency shift of transverse NMR in the c and f states of $^3\text{He-A}$ in aerogel according to Ref.³ Experiments with compensated deformation demonstrated the $(1 + \cos \beta)$ behavior similar to the f -line¹⁵

3.2 Tipping angle dependence of NMR

Lines c and f in the spectrum of transverse NMR in $^3\text{He-A}$ in aerogel demonstrate different dependence of frequency shift on the tipping angle β in Fig. 5. This can be compared with the theoretical frequency shift in the limit of the almost completely disordered state, when $L_{\text{LIM}}/\xi_D \ll 1$:

$$\frac{\Delta\omega(\beta)}{\Delta\omega_{\text{max}}} = b \cos \beta + a(1 + \cos \beta). \quad (10)$$

Here $\Delta\omega_{\text{max}}$ is the maximum possible frequency shift occurring in the uniform $\hat{\mathbf{I}}$ -field, it coincides with the magnitude of the negative frequency shift when $\hat{\mathbf{I}} \parallel \mathbf{H}$; the parameter $a \ll 1$ and $b \ll 1$ are nonzero due to the deviations from the full disorder caused by spin-orbit interaction¹⁶:

$$b = \frac{1}{2}(1 - 3\langle I_z^2 \rangle), \quad a = \frac{1}{6}(1 - 2\langle \sin^2 \Phi \rangle), \quad (11)$$

and Φ is the angle between the components $\hat{\mathbf{I}}_{\perp}$ and $\hat{\mathbf{d}}_{\perp}$, which are transverse to magnetic field $\mathbf{H} \parallel \hat{\mathbf{z}}$. Parameters a and b are zero in the limit when disorder is strong compared to the spin-orbit interaction, i.e. when $L_{\text{LIM}}/\xi_D \rightarrow 0$, and are proportional to $(L_{\text{LIM}}/\xi_D)^2$ with pre-factors depending on the type of disorder.

The disorder can be described in the following phenomenological way. In the c -state the transverse component $\hat{\mathbf{I}}_{\perp}$ of the vector $\hat{\mathbf{I}}$ is random, while the spin-space vector $\hat{\mathbf{d}}$ is perpendicular to \mathbf{H} and is regular. This gives $a = 0$. On the other hand the magnetic field $\mathbf{H} \parallel \hat{\mathbf{z}}$, via the vector $\hat{\mathbf{d}}$, produces a weak easy-plane anisotropy for the $\hat{\mathbf{I}}$ -vector. As a result, one has $b > 0$. The f -line represents regions with the f -state where the $\hat{\mathbf{I}}$ -vector is fully random, and thus $b = 0$, while $\hat{\mathbf{d}}$ and $\hat{\mathbf{I}}_{\perp}$ are not fully independent, producing $a > 0$.

However, it is not clear what is the microscopic background for such behavior of the parameters, and the detailed numerical simulations of the structure of different possible disordered states of $^3\text{He-A}$ in aerogel are required. Another interpretation of the β -dependence of the two NMR lines in terms of the modified robust phase has been proposed by Fomin¹⁷.

4 Discussion: superfluid properties of LIM state

In chiral anisotropic superfluids the LIM effect should influence the superfluid properties of the system. According to the Mermin-Ho relation in Eq.(3), circulation of superfluid velocity along the closed path L is expressed in terms of the surface integral over the $\hat{\mathbf{l}}$ -field

$$N(L) = \frac{1}{\kappa} \oint_L d\mathbf{r} \cdot \mathbf{v}_s = \frac{1}{4\pi} e^{ijk} \int_S dS_k \hat{\mathbf{l}} \cdot \left(\frac{\partial \hat{\mathbf{l}}}{\partial x^i} \times \frac{\partial \hat{\mathbf{l}}}{\partial x^j} \right). \quad (12)$$

Here we normalized the circulation to the circulation quantum in ${}^3\text{He}$, $\kappa = \pi\hbar/m$; the circulation number N is not necessarily integer in chiral superfluids.

If we ignore for a moment that the $\hat{\mathbf{l}}$ -field is the part of the order parameter triad $\hat{\mathbf{m}}$, $\hat{\mathbf{n}}$ and $\hat{\mathbf{l}}$ in Eq.(1) and consider $\hat{\mathbf{l}}$ as completely independent field, then the variance of N for sufficiently large contours is

$$\langle N^2(L) \rangle \sim \frac{L^2}{L_{\text{LIM}}^2}, \quad L \gg L_{\text{LIM}}. \quad (13)$$

This corresponds to randomly distributed skyrmions – vortices with continuous cores of the size L_{LIM} , which is also the mean distance between the skyrmions. Such a state resembles the plasma of vortices above the Berezinskii-Kosterlitz-Thouless transition, where vortices destroy superfluidity. This suggests that in aerogel, while the local superfluid density ρ_s on the scales below L_{LIM} is of the same order as in ${}^3\text{He-B}$, it could be reduced and even become zero at large scales.

Experiments on ${}^3\text{He-A}$ in aerogel^{18,19} demonstrate that $\rho_s \neq 0$ though it is somewhat smaller as compared to ρ_s in ${}^3\text{He-B}$. This shows that in the consideration of the LIM effect, we cannot ignore the energy of superflow – the energy related to the gradient $\hat{\mathbf{m}} \cdot \nabla \hat{\mathbf{n}}$, which is the superfluid velocity according to Eq.(3). It was stated that the energy of superflow is not relevant for the LIM effect²⁰. However, it should suppress the abundance of vortex-skyrmions. The pinning of skyrmions would also restore superfluidity.

There are many open questions related to the LIM state. In particular, how rigid is the $\hat{\mathbf{l}}$ -texture at large length scales and how strongly are the vortex-skyrmions pinned by aerogel? The problem of rigidity in the LIM state is thirty years old, see the paper by Efetov and Larkin²¹ and recent publications²². The idea of quasi-long-range order (QLRO) with a power-law decay of correlators discussed for a vortex lattice in superconductors²³ is applicable to ${}^3\text{He-A}$ in aerogel. Probably the QLRO does not occur in isotropic aerogel because of the non-Abelian $SO(3)$ group of triad $\hat{\mathbf{m}}$, $\hat{\mathbf{n}}$, $\hat{\mathbf{l}}$, but it should take place in a stretched aerogel where the easy plane anisotropy reduces $SO(3)$ to its Abelian $U(1) \times U(1)$ subspace. Following Ref.²⁴ one may expect that the power law is determined by relations between all 7 stiffness parameters K in the ${}^3\text{He-A}$ gradient energy⁶. The phase transition from LIM state with QLRO to the disordered LIM state or to the non-superfluid LIM state can be generated by increasing the density of skyrmions. The states c and f in NMR experiments³ and states in hydrodynamic experiments¹⁹ (see below) may differ by density of skyrmions and thus may have different superfluid properties.

The external superflow influences the LIM state due to anisotropy of the superfluid density in Eq.(2): since $\rho_{s\parallel} < \rho_{s\perp}$, the applied \mathbf{v}_s produces the global

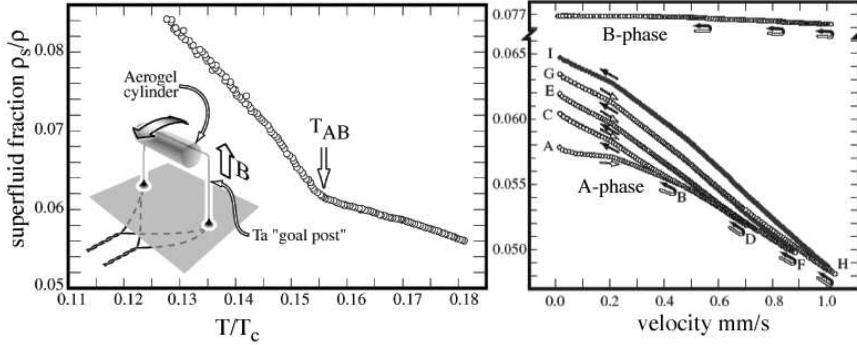


Fig. 6 Anisotropic superfluid density of $^3\text{He-A}$ in aerogel according to Ref. ¹⁹. Superfluid density is history dependent and depends on the applied superfluid velocity.

easy-axis anisotropy for $\hat{\mathbf{l}}$. This suggests that the sufficiently large \mathbf{v}_s destroys the LIM state, which is consistent with hydrodynamic experiment¹⁹ demonstrating glassy behavior of $\hat{\mathbf{l}}$ -texture at low \mathbf{v}_s and more regular behavior at large \mathbf{v}_s . If the initial state *A* in Fig. 6 is fully disordered but rigid, its superfluid density must be $\rho_s^A = (1/3)\rho_{s\parallel} + (2/3)\rho_{s\perp}$. With increasing \mathbf{v}_s the state becomes more and more uniform. In the state *H*, which is reached at large \mathbf{v}_s , the vector $\hat{\mathbf{l}}$ is oriented along \mathbf{v}_s , and one has $\rho_s^H = \rho_{s\parallel} < \rho_s^A$. Because of the hysteresis, the uniform texture persists when velocity is reduced, but now with $\hat{\mathbf{l}} \perp \mathbf{v}_s$ as dictated by geometry of the sample; as a result in the subsequent state *I* one has $\rho_s^I = \rho_{s\perp} > \rho_s^A$.

Another open problem is the role of extended objects. (i) Topological defects with hard cores (single-quantum and half-quantum vortices) may be pinned by aerogel. Trapping of singular vortices by aerogel has been observed in $^3\text{He-B}$ ⁵. This suggests that *c* and *f* states may have different abundance of defects. (ii) The network of connected aerogel strands may have the long-range correlations (e.g. due to elastic deformations of aerogel). The interplay of the quenched long-range and short-range disorder may also lead to two LIM states with different scales²⁵.

The LIM effect is rather subtle in $^3\text{He-A}$, it is destroyed by weak anisotropy produced by deformation of aerogel and/or by flow. This suggests that maybe the adequate description of the LIM effect is in terms of statistics of random deformations u_{ik} of aerogel with the energy term in Eq.(8), instead of the discussed statistics of random orientations of strands. On the other hand, the global anisotropy produced by sufficiently large deformations allows us to study novel phenomena which cannot be observed in bulk $^3\text{He-A}$. For example, orientation of $\hat{\mathbf{l}}$ along the magnetic field \mathbf{H} (not possible in a pure bulk $^3\text{He-A}$) stabilizes: (i) Alice strings (half-quantum vortices) in rotating sample²⁶; and (ii) the phase-coherent precession of magnetization²⁷ recently observed in a squeezed aerogel^{28,5}. The coherent precession in $^3\text{He-A}$ is another realization of Bose-Einstein condensation (BEC) of magnons. The first example of magnon BEC found in 1984 in $^3\text{He-B}$ is known as the homogeneously precessing domain (HPD, see reviews^{29,30}), and historically this was the first BEC which was experimentally stabilized. Magnon con-

densates in $^3\text{He-A}$ and condensates in $^3\text{He-B}$ (HPD, the state HPD_2 observed in a stretched aerogel³¹ and Q -balls³²) all have different spin-superfluid properties³⁰.

In conclusion, $^3\text{He-A}$ in aerogel is one of the most interesting objects for investigation of the Larkin-Imry-Ma and related effects.

Acknowledgements I thank Yu.M. Bunkov, V.V. Dmitriev, T. Giamarchi, T. Nattermann and Y. Tanaka for illuminating discussions, the Academy of Finland and the Russian Foundation for Fundamental Research (grant 06-02-16002-a) for support.

References

1. Yu.M. Bunkov *et al.*, *Phys. Rev. Lett.* **85**, 003456 (2000); *J. Phys. Chem. Solids* **66**, 1325 (2005).
2. Y. Tanaka and A.A. Golubov, *Phys. Rev. Lett.* **98**, 037003 (2007).
3. V.V. Dmitriev *et al.*, *JETP Lett.*, **84**, 461 (2006).
4. T. Kunimatsu *et al.*, *Pisma ZhETF* **86**, 244 (2007); arXiv:cond-mat/0612007.
5. T. Kunimatsu *et al.*, *J. Low Temp. Phys.*, this issue.
6. D. Vollhardt and P. Wölfle, *The superfluid phases of helium 3*, Taylor and Francis, London (1990).
7. N.D. Mermin and Tin-Lun Ho, *Phys. Rev. Lett.* **36**, 594 (1976).
8. Y. Imry and S.K. Ma, *Phys. Rev. Lett.* **35**, 1399 (1975).
9. A.I. Larkin, *JETP* **31**, 784 (1970).
10. C.L. Vicente *et al.*, *Phys. Rev. B* **72**, 094519 (2006).
11. G.E. Volovik, *JETP Lett.* **63**, 301 (1996).
12. E.V. Surovtsev and I.A. Fomin, arXiv:0708.1074.
13. D. Rainer and M. Vuorio, *J. Phys.* **10**, 3093 (1977).
14. K. Aoyama and R. Ikeda, *Phys. Rev. B* **73**, 060504(R) (2006).
15. V.V. Dmitriev *et al.*, arXiv:0709.3180
16. G.E. Volovik, *JETP Lett.*, **84**, 455 (2006).
17. I.A. Fomin, *JETP Lett.*, **84**, 624 (2006).
18. E. Nazaretski, N. Mulders and J. M. Parpia, *JETP Lett.* **79**, 383 (2004).
19. D.I. Bradley *et al.*, *Phys. Rev. Lett.* **98**, 075302 (2007).
20. K. Aoyama and R. Ikeda, *Phys. Rev. B* **73**, 012515 (2005).
21. K. Efetov and A.I. Larkin, *JETP* **45**, 1236 (1977).
22. M. Itakura, *Phys. Rev. B* **68**, 100405 (2003); D.E. Feldman and R.A. Pelcovits, *Phys. Rev. E* **70**, 040702(R) (2004); B.M. Khasanov, *JETP Lett.* **81**, 24 (2005); J. Wehr *et al.*, cond-mat/0604063; T. Emig and T. Nattermann, cond-mat/0604345; L. Petridis and E.M. Terentjev, cond-mat/0610010.
23. T. Giamarchi and P. Le Doussal, *Phys. Rev. B* **52**, 1242 (1995).
24. T. Emig, S. Bogner and T. Nattermann, *Phys. Rev. Lett.* **83**, 400 (1999).
25. A.A. Fedorenko and F. Kühnel, *Phys. Rev. B* **75**, 174206 (2007).
26. M.M. Salomaa and G.E. Volovik, *Rev. Mod. Phys.* **59**, 533 (1987).
27. Yu.M. Bunkov and G.E. Volovik, *Europhys. Lett.* **21**, 837 (1993).
28. T. Sato *et al.*, to be published.
29. G.E. Volovik, arXiv:cond-mat/0701180.
30. Yu.M. Bunkov and G.E. Volovik, arXiv:0708.0663.
31. J. Elbs *et al.*, arXiv:0707.3544.
32. Yu.M. Bunkov and G.E. Volovik, *Phys. Rev. Lett.* **98**, 265302 (2007).